Progress in Oceanography 97–100 (2012) 92–107

Contents lists available at SciVerse ScienceDirect

Progress in Oceanography

journal homepage: www.elsevier.com/locate/pocean

The influence of phytoplankton productivity, temperature and environmental stability on the control of copepod diversity in the North East Atlantic

Enrique Nogueira *, Gonzalo González-Nuevo, Luis Valdés [1]

Instituto Español de Oceanografía, Centro Oceanográfico de Gijón, Avda. Príncipe de Asturias 70bis, 33212 Gijón, Spain

ARTICLE INFO

Article history:
Available online 19 November 2011

ABSTRACT

The patterns of copepod species richness (S) and their relationship with phytoplankton productivity, temperature and environmental stability were investigated at climatological, seasonal and year-to-year time scales as well as scales along latitudinal and oceanic–neritic gradients using monthly time series of the Continuous Plankton Recorder (CPR) Survey collected in the North East Atlantic between 1958 and 2006. Time series analyses confirmed previously described geographic patterns. Equatorward and towards neritic environments, the climatological average of S increases and the variance explained by the seasonal cycle decreases. The bi-modal character of seasonality increases equatorward and the timing of the seasonal cycle takes place progressive earlier equatorward and towards neritic environments. In the long-term, the climatological average of S decreased significantly ($p < 0.001$) between 1958 and 2006 in the Bay of Biscay and North Iberian shelf at a rate of ca. 0.04 year^{-1}, and increased at the same rate between 1991 and 2006 in the northernmost oceanic location. The climatological averages of S correlate positively with those of the index of seasonality of phytoplankton productivity (ratio between the minimum and maximum monthly values of surface chlorophyll) and sea surface temperature, and negatively with those of the proxy for environmental stability (monthly frequency of occurrence of daily averaged wind speed exceeding 10 m s^{-1}). The seasonal cycles of S and phytoplankton productivity (surface chlorophyll as proxy) exhibit similar features in terms of shape, timing and explained variance, but the relationship between the climatological averages of both variables is non-significant. From year-to-year, the annual averages of S correlate negatively with those of phytoplankton productivity and positively with those of sea surface temperature along the latitudinal gradient, and negatively with those of environmental stability along the oceanic–neritic gradient. The annual anomalies of S (i.e. factoring out geographic variation) show a unimodal relationship with those of sea surface temperature and environmental stability, with S peaking at intermediate values of the anomalies of these variables. The results evidence the role of seasonality of phytoplankton productivity on the control of copepod species richness at seasonal and climatological scales, giving support to the species richness–productivity hypothesis. Although sea surface temperature (SST) is indeed a good predictor of richness along the latitudinal gradient, it is unable to predict the increase of richness form oceanic to neritic environments, thus lessening the generality of the species richness–energy hypothesis. Meteo-hydrographic disturbances (i.e. SST and wind speed anomalies as proxies), presumably through its role on mixed layer depth dynamics and turbulence and hence productivity, maximise local diversity when occurring at intermediate frequency and or intensity, thus providing support to the intermediate disturbance hypothesis on the control of copepod diversity.

© 2011 Elsevier Ltd. All rights reserved.

1. Introduction

The study of the patterns of species richness and their causes is one of the central and oldest questions in ecological and evolutionary theory (Darwin, 1839). The latitudinal, equatorward increase in species richness has received much attention. This pattern has being reported for an ample number of taxa independently of the geographic context (terrestrial or oceanic) or time domain (contemporary or paleontological) considered (Willing et al., 2003). However, while the patterns have become increasingly well documented, especially in the last decade due to the concerns about the impacts of global change on the erosion of diversity and its effect on ecosystem function and dynamics (Chown and Gaston, 2000; Worm et al., 2006), the relative importance of the factors and mechanisms proposed to account for the temporal and spatial changes of diversity remains a matter of debate (Willing et al., 2003; Mora and Robertson, 2005). Most causal

* Corresponding author. Tel.: +34 985308672; fax: +34 985326277
E-mail address: enrique.nogueira@gi.ieo.es (E. Nogueira).
[1] Present address: Intergovernmental Oceanographic Commission, UNESCO, 1 Rue de Miollis, 75732 Paris, France.

0079-6611/$ - see front matter © 2011 Elsevier Ltd. All rights reserved.
doi:10.1016/j.pocean.2011.11.009

hypotheses can be classified into those based on the variability of environmental factors (productivity, energy supply and environmental stability), null models (the mid-domain effect) or other patterns, such as the Rapoport effect (Rohde, 1992; Roy et al., 1998; Colwell and Lees, 2000).

The knowledge of diversity patterns in the pelagic realm is still scarce compared to that for terrestrial ecosystems (Hillebrand, 2004; Webb, 2009). It has being suggested that species richness varies along latitudinal, oceanic–neritic and bathymetric gradients (Angel, 1997). Proposed explanations to account for present day patterns invoke numerous interacting factors which operate on a wide range of spatial and temporal scales, from global/geological (10^4 km/millennia) to local/diel (metres/hours) (Angel, 1997). The co-variability observed between species richness of different pelagic taxa and environmental descriptors, such as sea surface temperature, concentration of inorganic nutrients or chlorophyll, gives support to the hypotheses that stress the role of environmental factors as controllers of diversity. Among them, the species richness–ambient energy and the species richness–productivity hypotheses (Currie, 1991; Willing et al., 2003) have received the greatest support among pelagic taxa (e.g. Roy et al., 1998; Rutherford et al., 1999; Macpherson, 2002; Rombouts et al., 2009). The ambient energy hypothesis states that the input of solar energy determines a physical environment that affects organisms through their physiological responses to temperature. This hypothesis includes other explanations, such as climatic stability, environmental stability, environmental predictability, seasonality and harshness (Willing et al., 2003). The productivity hypothesis posits that energy availability, productivity and biomass, also tightly linked to the input of solar energy, are the main controllers of diversity. Both hypotheses share the common theme of energy but differ in the ultimate pathways by which available energy controls diversity. Gillooly and Allen (2007) suggest that the two forms of energy, kinetic and chemical potential energy, should be kept separate because they regulate diversity in different ways: the first through its effects on metabolic rates, the second through its effects on total community abundance. Discrimination between hypotheses is complicated by the multi-factorial and multi-scale control of diversity (Angel, 1997) and by the potential bias induced by spatial autocorrelation and co-linearity among environmental explanatory variables (Mora and Robertson, 2005; Rombouts et al., 2009), which makes it difficult to determine which of the environmental factors are causal or coincidental (Colwell and Lees, 2000).

Among the biotic components of the pelagic ecosystem, zooplankton play a fundamental role because of their importance in terms of both abundance and biomass and their contribution to a variety of ecosystem processes (Richardson, 2008). Copepods, the most prominent taxa of zooplankton, act as major grazers in oceanic food-webs, channelling energy from primary producers to higher trophic levels, and contribute to biogeochemical cycles by means of the regeneration of nutrients through excretion and the sequestration of organic matter into the seafloor via sinking of faecal pellets and corpses, thus contributing in a fundamental way to the biological pump (Longhurst and Harrison, 1989). In addition, copepods are also good indicators of climate change because their growth, reproduction and distribution are under strong bottom-up control (Mauchline, 1998; Richardson, 2008). Consequently, knowledge of the patterns of copepod diversity, both at regional and basin scales, and the underlying factors and mechanisms controlling their patterns of distribution and diversity is fundamental in the present scenario of global change (i.e. over exploitation, pollution and climate change – deYoung et al., 2008; Cury et al., 2008). Whereas the patterns of copepod diversity have been documented in recent years at several temporal and spatial scales (Beaugrand et al., 2000a, 2002b; Wood-Walker, 2001, 2002; Piontkovski et al., 2006; Rombouts et al., 2009), the investigation on the environmental controls has received less attention (Beaugrand et al., 2000a, 2003; Beaugrand and Ibanez, 2004; Rombouts et al., 2009).

The Continuous Plankton Recorder (CPR) Survey (http://www.sahfos.org/) provides the scientific community long-term, near-surface abundance of phyto- and zooplankton data in the North Atlantic (Richardson et al., 2006). The application of time series, multivariate and geostatistical techniques to different spatial and temporal aggregations of CPR data have provided new insights on the distribution of copepod diversity in the North Atlantic and the hydroclimatic factors that control its spatial (from meso- to basin-scale) and temporal (from daily to multi-decadal) variability (Beaugrand et al., 2000a, 2000b, 2001, 2002a, 2003; Beaugrand, 2004a,b). Here we have applied time series analysis techniques to spatial compartments (selected CPR Standard Areas) (Beare et al., 2003 and references therein) distributed along oceanic, latitudinal and temperate, oceanic–neritic gradients in the North East Atlantic to: (1) characterise the patterns of copepod species richness at climatological, seasonal and year-to-year time scales along these gradients, and (2) analyse the relationship between copepod species richness and phytoplankton productivity, temperature and environmental stability to investigate the role of these factors on the control of copepod diversity.

2. Material and methods

2.1. Indices of copepod species richness from CPR data

The CPR Survey, initiated in 1931 by Sir Alister Hardy (Hardy, 1939), is the largest plankton monitoring programme in the world (Reid et al., 2003). Sampling is carried out by means of a high speed plankton recorder device towed by 'ships of opportunity' along their standard routes (Hays, 1994; Warner and Hays, 1994; Reid et al., 2003). Each sample corresponds to approximately 3 m^3 of near-surface (ca. 7 m depth) seawater filtered by a slow moving band of silk of 270 μm mesh size along ca. 10 nautical miles of tow (Hays, 1994). Methods of counting and data processing, which have been consistent since 1948 (Batten et al., 2003), are described in detail elsewhere (Richardson et al., 2006).

For the present study we have selected eight CPR Standard Areas in the North East Atlantic covering a latitudinal range from 40° to 67°N: B6 to F6 are distributed along an oceanic, latitudinal gradient (centred at 25°W and 61.5°, 57.0°, 52.5°, 47.5° and 42.5°N respectively), while F6–F4 and E4 cover from oceanic to neritic, temperate domains (centred at 42.5°N, 15°W; 44.0°N, 6.5°W; and 46.5°N, 6.5°W for F5, F4 and E4 respectively) (Fig. 1). The selected CPR Standard Areas extend over three types of North Atlantic biomes (Longhurst, 1998): polar (Subarctic province, SARC; B6), westerly winds (North Atlantic Drift and North Atlantic Subtropical Gyral provinces, NADR and NAST; C6–F6) and coastal (North East Atlantic Shelves, NECS; E4 and F4). In terms of the communities of copepod species, four main types are present within the study area (Beaugrand et al., 2002a; Beaugrand and Ibañez, 2002): subarctic (B6–D6), cold-temperate (D6–E6), warm-temperate (F6–F5) and Bay of Biscay and southern European shelf edge (E4–F4) communities.

We used the mean taxonomic richness per sample (S) as defined by Beaugrand et al. (2000b) as an index of copepod species richness. Monthly time series of S were obtained by averaging the number of calanoid copepod categories (from a list of 106 categories) in individual samples collected each month between 1958 and 2006 within the limits of the selected CPR Standard Areas (Supplementary material). The samples were averaged monthly irrespective of their spatial (i.e. position within each Area) and temporal (i.e. time of the day of collection) heterogeneity (Beaugrand et al., 2001).

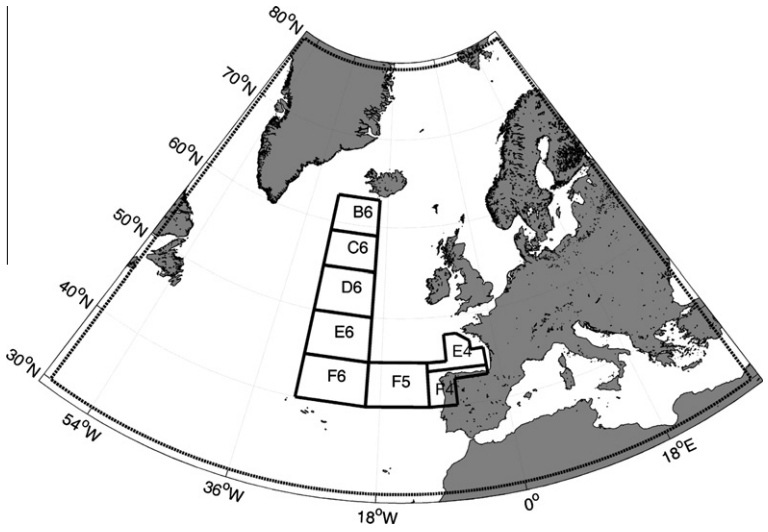

Fig. 1. Map of the study area showing the position of the Continuous Plankton Recorder (CPR) Standard Areas selected for the presented study; B6–F6 are distributed along an oceanic, latitudinal gradient while F5–F4 and E4 are representative of a temperate, oceanic–neritic gradient.

We calculated the total richness per month (S_{ac}), that is, the monthly cumulative number of different copepod categories from the individual samples obtained in a given month of the time series. For each of the selected areas we have constructed species-samples (or accumulation) curves (Gotelli and Colwell, 2001) from the relationship between the total richness per month (S_{ac}) and the volume sampled by the CPR (V, m^3) that month. We assumed that the relationship between S_{ac} and V follows a saturating function, to which we fitted a Michaelis–Menten (M–M) function. The asymptotic value of the M–M function (S_{ac_max}) provides an estimation of the maximum richness sampled by the CPR.

2.2. Environmental data: surface chlorophyll and meteo-hydrographic variables

Satellite-derived surface chlorophyll concentration, an indicator of phytoplankton standing stock, was used as a proxy for ocean productivity (Macpherson, 2002). Monthly time series of surface chlorophyll concentration (Chl, mg m^{-3}) for each CPR Standard Area were derived from SeaWiFS (level 3) monthly values mapped at ca. $9 \times 9\ km^2$ pixels between 1998 and 2008 (http://oceancolor.gsfc.nasa.gov/) (Supplementary material). From these time series we calculated the ratio between the minimum and maximum monthly averaged chlorophyll, for each year and for the seasonal cycle. This ratio quantifies the amplitude of the seasonal signal of chlorophyll relative to its baseline, and is thus an index of the seasonality of phytoplankton standing stock (SPSS): high (low) values of the SPSS index are indicative of low (high) amplitude seasonal cycles.

Sea surface temperature (SST, °C) and the number of days per month with daily averaged wind speed exceeding 10 m s^{-1} (w10, days $month^{-1}$) were selected as descriptors of the meteo-hydrographic environment and proxies for energy availability and environmental stability respectively. Monthly time series of SST and w10 for each CPR Standard Area (Supplementary material) were calculated from monthly SST and daily wind speed data averaged over each Standard Area (grid resolution: 2° and 2.5° for SST and wind speed respectively). These data were retrieved from the Earth System Research Laboratory web page (http://www.cdc.noaa.gov/).

2.3. Numerical analysis

We have applied time series analysis techniques to decompose and parameterise the multi-year (linear and cyclical), seasonal and random components of variation of the mean taxonomic richness per sample (S) and environmental variables (Chl, SST and w10). Gaps in the monthly time series of S and Chl were filled with the respective monthly average of the seasonal cycle. Time series analysis methods have been already applied by several authors to CPR data (e.g. Broekhuizen and McKenzie, 1995; Rothschild, 1998; Beare and McKenzie, 1999; Kirby et al., 2009). The relationships among variables were explored using linear and non-linear regression techniques. All the analyses were performed using Matlab®.

We fitted an additive decomposition model to the time series in order to parameterize the main modes of temporal variability,

$$x_t = \bar{x} + LT[x_t] + LTC[x_t] + SC[x_t] + R[x_t] \quad (1)$$

where t is the index for time; $\bar{x}$, the climatological average of the variable analysed; LT is the long-term linear trend; LTC and SC represent the multi-year and seasonal cyclical components respectively; and R accounts for the remaining fluctuations of the time series. LT, LTC and SC were treated as 'deterministic' components (Chatfield, 1992).

The seasonal component was defined by the combination of the first and second harmonics of the annual period,

$$SC[x_t] = A_{12}\cos\left(\frac{2\pi}{12}t + \theta_{12}\right) + A_6\cos\left(\frac{2\pi}{6}t + \theta_6\right) \quad (2)$$

where A_{12} and A_6 are the amplitudes of the first (period, T = 12 months) and second (T = 6 months) harmonics of the annual period respectively, and θ_{12} and θ_6 are their phases in radians. These parameters were extracted by means of Fourier analysis (Poularikas and Seely, 1991). The timing of the seasonal cycle was specified by the month when the maximum of a given cycle occurs (T_m):

$$-\theta_i = \frac{2\pi}{T_i}T_m \quad (3)$$

The long-term variation was parameterized by the slope of the linear trend and/or the amplitude, phase and period of long-term cycles (T > 12 months). The statistical significance level of the extracted cycles was estimated according to the Anderson criterion (A_c) (Legendre and Legendre, 1998):

$$A_c = -(2/n)log_e(1 - \sqrt[m]{1-\alpha}) \quad (4)$$

where n is the number of observations in the series, m is the largest computed harmonic period, and α is the probability level.

The 'stochastic' component, the de-trended and de-seasonalized residuals, was parameterized by means of an autoregressive model, which involves the description of the time series in terms of a weighted sum of its own past values,

$$R[x_t] = \phi_i(R[x_{t-i}]) + a_t \quad (5)$$

where ϕ_i are the auto-regressive parameters, and a_t represents the pre-whitened residuals, a time series of independent, identical and normally distributed random shocks (or white noise) with zero mean and constant variance (σ_a^2). The order of the autoregressive process is defined by the inspection of the auto-correlation (acf) and partial auto-correlation functions (pacf), and the auto-regressive parameters were estimated using the Yule–Walker equations (Wei, 1990).

We plotted the parameters of the fitted univariate models (average, amplitude and timing of 1st and 2nd harmonics of the annual period, slope of the linear trend and first-order autoregressive parameter) relative to the latitudinal and oceanic–neritic gradients to highlight the geographic patterns of copepod diversity and environmental conditions along these gradients.

The relationships between the mean taxonomic richness per sample (S) and the environmental variables were analysed at climatological and year-to-year scales, for the annual averages (Eq. (6.1)) and annual residuals (Eq. (6.2)) (i.e. factoring out the geographic patterns), to test the role of ocean productivity (Chl and SPSS), energy availability (SST) and environmental stability (w10 and annual residuals of SST and w10) as underlying factors regulating S:

$$\bar{S}_{j(i>6),k} : f(\bar{x}_{j,k}) \quad (6.1)$$

$$\Delta S_{j,k} : f(\Delta x_{j,k}), \text{ being } \Delta S_{j,k} = \bar{S}_{j(i>6),k} - \bar{S}_k \text{ and } \Delta x_{j,k} = \bar{x}_{j,k} - \bar{x}_k \quad (6.2)$$

where j, i and k are the sub-indices for year, month and CPR Standard Area respectively, and x designates the environmental variables. To reduce biases in the estimation of the annual averages of S we have considered only those years with more than six sampled months ($i > 6$). Prior to the analysis, the annual time series were de-trended (i.e. trend subtraction) if necessary to make them stationary. The relationships between the de-trended annual time series of S and environmental descriptors were explored using linear, curvilinear or locally weighted polynomial regression (loess function) (Cleveland and Devlin, 1988). For loess regression, at each point in the data set a 2nd degree (quadratic) polynomial was fitted to a subset of the data, with values of the explanatory variable near to the point whose response is being estimated. The smoothing parameter (α) was chosen taking into account the dispersion of the data to be fitted; α was set between 0.2 and 0.3, within the typical range for applications of the loess function.

3. Results

3.1. Geographic patterns

3.1.1. Mean taxonomic richness (S)

Along the oceanic, latitudinal gradient, the climatological average of mean taxonomic richness of copepods per sample (S) increased equatorward (Fig. 2a). Seasonality was a prominent mode of variation in the monthly time series, although its contribution to total variability decreased from subpolar to temperate latitudes (ca. 65% in B6–C6 to ca. 40–50% in E6–F6) (Table 1). The seasonal cycle showed a marked latitudinal pattern (Fig. 3a): the unimodal character of the cycle was significantly higher in subpolar than in temperate latitudes (steep change in A_{12} between B6–C6 and D6–F6), while the relevance of the semi-annual component increased equatorward (rising A_6:A_{12} ratio from 0.2 to 1.7 between B6 and F6). Seasonally, S peaked on average in spring (April–May) and to a lesser extent in autumn (October) in the temperate locations of the gradient (E6 and F6), while at the northernmost side (B6 and C6) a single but extended summer peak of S occurred about two months later (from June to September). In the long-term S decreased in C6, although the slope of this decreasing trend was only marginally significant ($p < 0.05$ in the de-seasonalized time series) and its estimation must be taking with caution due to the discontinuity of the series (Supplementary material). If we considered continuously sampled intervals in the series, S decreased slightly in the northernmost location (B6) between 1958 and 1986 but increased conspicuously in the last decade (1991–2006) (annual rates: −0.01 and 0.04 S year^{-1} respectively; $p < 0.05$ in both cases). The de-trended and de-seasonalized residuals presented a significant autocorrelation only for the time series of B6 (Table 1). The autocorrelation coefficient was lower for the subset of the time series (r at lag $k = 1$, $r_1 = 0.17$ and 0.15 for the first and second sub-set respectively) than for the complete series ($r_1 = 0.22$), indicating that for this last case the serial dependence captures de long-term variability of each of the time series subsets (Table 1).

The average of S increased along the temperate, oceanic–neritic gradient from ca. 2.0 in the oceanic side (F6 and F5) to 3.4 and 4.1 in the more neritic areas (E4; Bay of Biscay and F4; North Iberian shelf). The amount of variance retained by the seasonal cycle was significantly lower in neritic (ca. 34% and 28% in E4 and F4 respectively) than in oceanic environments. The bimodality of the seasonal cycle characterised all CPR Standard Areas along this gradient, although the spring and autumn peaks of S happened earlier in the neritic areas (E4–F4) (March–April and September–October) (Fig. 3b). The time series for E4 and F4 showed a decreasing, highly significant ($r = -0.31$ and -0.23 respectively, $p < 0.001$ both) long-term trend (ca. −0.04 S year^{-1}). Autocorrelation was also significant in these series.

3.1.2. Phytoplankton standing stocks (Chl)

The climatological average of surface chlorophyll from SeaWiFS (Chl) was higher at northern locations (B6–D6) than at southern ones (E6–F6) (Fig. 2b). The contribution of the seasonal cycle decreased equatorward from 63% in B6 to 41% in F6 (Table 2). The amplitude of the annual component decreased, the bimodality of the seasonal cycle increased and the peaks of phytoplankton standing stock occurred earlier equatorward. At southern locations (E6–F6), the spring peak took place in April–May and the autumn peak in October–November, while at northern locations (B6–D6) a single peak occurred between May and July (Fig. 3c). Only at the southern locations (E6–F6) surface chlorophyll decreased significantly between 1998 and 2008 ($r = -0.27$, $p < 0.01$ and $r = -0.28$, $p < 0.001$ respectively) at a rate of −0.01 to −0.02 mg Chl m^{-3} year^{-1}. All the series showed significant autocorrelation, for which the contribution to total variance ranged from 3.5% to 15.7% for B6 and F6 respectively.

Along the oceanic–neritic gradient, the climatological average of surface chlorophyll (Chl), the amplitudes of the annual and semi-annual components and the bimodality of the seasonal cycle, which accounted for a percentage of variance ranging between 40% and 60%, increased towards neritic areas. Also, the spring and autumn peaks occurred progressively earlier in neritic environments than in oceanic ones: May–November in F6, April–October in E4 and March–September in F4 (Fig. 3d). F5 and F4 showed marginally significant ($p < 0.05$) long-term trends of different sign (ca. −0.01 and 0.01 mg Chl m^{-3} year^{-1} respectively). All the series exhibited significant autocorrelation.

3.1.3. Meteo-hydrographic conditions (SST and w10)

Sea surface temperature (SST) showed an increasing pattern equatorward for most of the univariate time series model

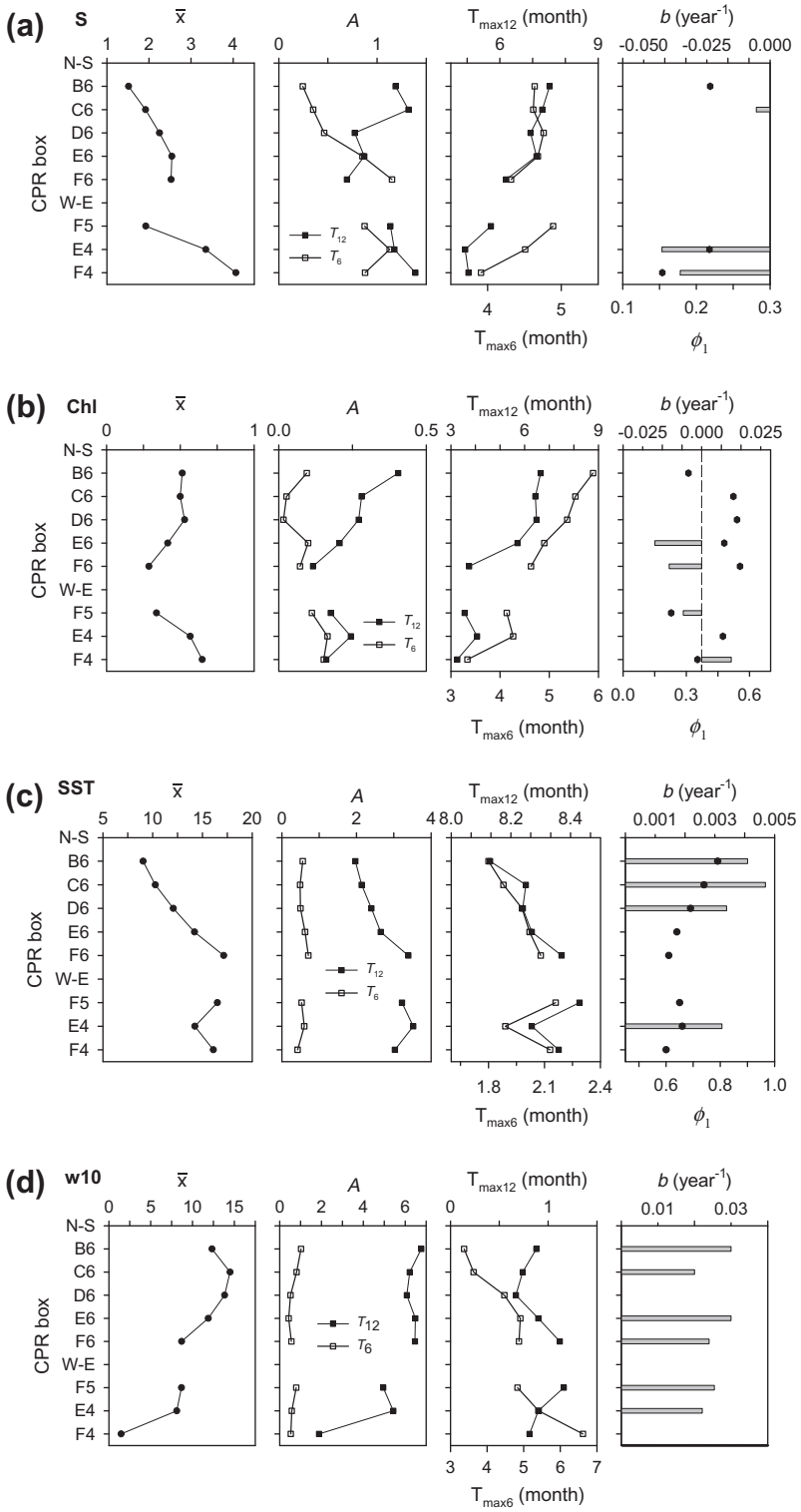

Fig. 2. Charts of the variability of the parameters of the univariate time series models fitted to the monthly time series along the latitudinal (B6–F6) and oceanic–neritic (F6–F4 and E4) gradients (Tables 1 and 2): (a) copepod species richness (*S*, mean number of copepod categories per CPR sample); (b) surface chlorophyll from SeaWiFS (Chl, mg m^{-3}); (c) sea surface temperature (SST, °C); (d) number of days per month with daily average wind speed exceeding 10 m s^{-1} (w10, days·mo^{-1}). The parameters of the time series models are, from left to right: climatological average ($\bar{x}$), amplitude of the first (A_{12}, black square) and second (open square) harmonics of the annual period (A_6); phase of A_{12} and A_6, indicated as the month of the year when the maximum of each cyclical component occurs (T_{max12} and T_{max6}, top and bottom *x*-axis respectively); slope of the linear trend (*b*, as the rate of change per year) (bars, top *x*-axis); and value of the first-order autoregressive parameter (Φ_1) (black dots, bottom *x*-axis).

parameters (Fig. 2c). The climatological average of SST increased from 9.0 °C in B6 to 17.1 °C in F6 (Table 2). The amplitude of the annual component, which accounted for a percentage of variance between 84% (B6) and 91% (F6), differed by 1.4 °C between the extreme locations of the latitudinal gradient. The timing of the annual and semi-annual components occurred progressively later (between 7 and 10 days) equatorward. Maximum values in the seasonal cycle were observed in August. In the northern areas

Table 1
Parameters of the univariate time series models fitted to the monthly time series of mean copepod species richness per sample (S) in different CPR Standard Areas (CPR Area) for the whole length of the series (shaded grey rows) and for subsets of relatively continuous sampling (see Supplementary material) (not applicable for F5 due to scarcity of data in the subsets). Var, variable (S); Years, period analysed; n, number of samples and number of sampled months (mo); $\bar{x}$, climatological average; b, slope of the linear trend (year^{-1}); T, A, F and T_m are the period, amplitude, phase (in radians) and month of the maximum for the 1st and 2nd harmonics of the annual period; ϕ_1, the value of the first order autoregressive parameter (lag $k = 1$); EV_{LT}, EV_{SC}, EV_{AR} and EV_T are respectively the percentages of variance explained (i.e. coefficient of determination, r^2) by the long-term, seasonal and auto-regressive components and by the resultant univariate additive decomposition model.

Var	CPR Area	Years	n mo	$\bar{x}$	b	EV_{LT}	T	A	F	T_m	EV_{SC}	ϕ_1	EV_{AR}	EV_T
S	B6	1958–2006	7969	1.51			12	1.19	2.35	7.5	63.5	0.22	1.6	67.8
			453				6	0.24	1.43	4.6	2.7			
		1958–1986	6060	1.50	−0.01	1.3	12	1.12	2.32	7.6	58.0	0.17	1.1	64.6
			298				6	0.30	1.52	4.6	4.2			
		1991–2006	1909	1.55	0.04	2.3	12	1.33	2.39	7.4	69.1	0.15	0.5	72.9
			155				6	0.16	1.05	5.0	1.0			
	C6	1958–2006	1544	1.92	−0.01	0.3	12	1.32	2.46	7.3	59.0			63.4
			162				6	0.35	1.45	4.6	4.1			
		1958–1986	949	2.12			12	1.49	2.27	7.7	66.7			71.5
			87				6	0.40	1.26	4.8	4.8			
		1988–2006	595	1.72			12	1.21	2.71	6.8	46.7			50.2
			75				6	0.33	1.71	4.3	3.5			
	D6	1958–2006	3091	2.25			12	0.77	2.65	6.9	20.9			28.4
			231				6	0.46	1.30	4.8	7.5			
		1958–1986	1934	2.33			12	0.75	2.56	7.1	18.8			27.3
			149				6	0.50	0.99	5.1	8.5			
		1994–2006	1157	2.09			12	0.81	2.81	6.6	17.4			22.9
			82				6	0.46	1.82	4.3	5.5			
	E6	1967–2006	3304	2.54			12	0.87	2.55	7.1	20.8			40.8
			189				6	0.85	1.38	4.7	19.9			
		1967–1985	1752	2.85			12	0.72	2.39	7.4	11.0			36.4
			108				6	1.10	1.29	4.8	25.4			
		1997–2006	1552				12	1.10	2.74	6.8	27.0			36.5
			81				6	0.65	1.84	4.2	9.5			
	F6	1970–2006	2418	2.53			12	0.69	3.04	6.2	14.1			52.9
			141				6	1.15	1.76	4.3	38.9			
		1970–1982	1419	2.39			12	0.85	3.32	5.7	16.7			47.0
			82				6	1.15	1.62	4.5	30.3			
		1998–2006	999				12	0.70	2.33	7.6	10.5			32.4
			59				6	1.01	1.97	4.1	21.9			
	F5	1967–2006	471	1.92			12	1.14	3.29	5.7	29.3			46.5
			64				6	0.87	1.16	4.9	17.3			
		1967–1982	213	2.09										
			36											
		2000–2006	258	1.48										
			28											
	E4	1958–2006	6557	3.35	−0.04	9.4	12	1.18	3.70	4.9	17.9	0.22	2.7	46.6
			515				6	1.13	1.56	4.5	16.5			
	F4	1958–2006	2677	4.06	−0.04	5.2	12	1.39	3.64	5.0	20.0	0.15	1.5	34.8
			357				6	0.88	2.19	3.9	8.0			
		1958–1990	1580	4.39	−0.05	4.0	12	1.38	3.47	5.4	18.5	0.16	2.0	30.9
			261				6	0.82	2.23	3.9	6.5			
		1998–2006	1097	3.18			12	1.54	4.02	4.3	23.8			37.1
			96				6	1.15	2.01	4.1	13.3			

(B6–D6) the series exhibited significant long-term increasing trends (between 0.003 and 0.004 °C year^{-1}). A significant ($p < 0.05$ according to Anderson criterion) multi-year cycle was extracted from the series at the northernmost latitudes (B6–C6). These long-term components represent about 3% of the variability of the series and according to their respective phases depicted a cycle that reached minimum values in the mid eighties (1983–1984). All the series exhibited significant autocorrelation, although its contribution to total variance decreased from boreal (4.1% in B6) to sub-tropical latitudes (1.3% in F6).

At temperate locations along the oceanic–neritic gradient, the climatological average of SST decreased slightly from F6 (17.1 °C) towards neritic environments (F4, 16.1 °C), descending to 14.2 °C in the Bay of Biscay area (F4). The seasonal component accounted for more than 90% of the variance in all temperate locations, and the amplitudes of the annual and semi-annual components were similar all along the gradient (Table 2). The seasonality differed only in the timing: the seasonal peak occurred around 1 week earlier in the neritic side. E4 showed an increasing, marginally significant, long-term trend of 0.003 °C year^{-1}. All the series exhibited significant autocorrelation, although its contribution to total variance was minor (ca. 1%).

The climatological average of the number of days per month with daily averaged wind speed exceeding 10 m s^{-1} (w10) was higher at intermediate (ca. 14 days·month^{-1} in C6–D6) than in the extreme locations (ca. 12 and 9 days·month^{-1} in B6 and F6 respectively) of the latitudinal gradient (Fig. 2d). The seasonal cycle represented between 54% and 64% of the variability of the series. It shape, strongly unimodal (A_6:A_{12} ca. 0.1), was similar through the studied latitudinal range except for the timing, which was delayed ca. 14 days equatorward (seasonal peaks in late January and early February in B6 and F6 respectively). All the series except D6 showed an increasing long-term trend (annual rate ca. 0.03 days month^{-1} year^{-1}). None of the series showed significant autocorrelation (Table 2).

At temperate latitudes, the climatological average and the amplitudes of the components of the seasonal cycle of w10 were significantly lower in the most neritic environment (F4). The seasonal cycle, which was mainly unimodal (A_6:A_{12} ca. 0.1–0.2), accounted for 55% and 35% of the variability of the series in the

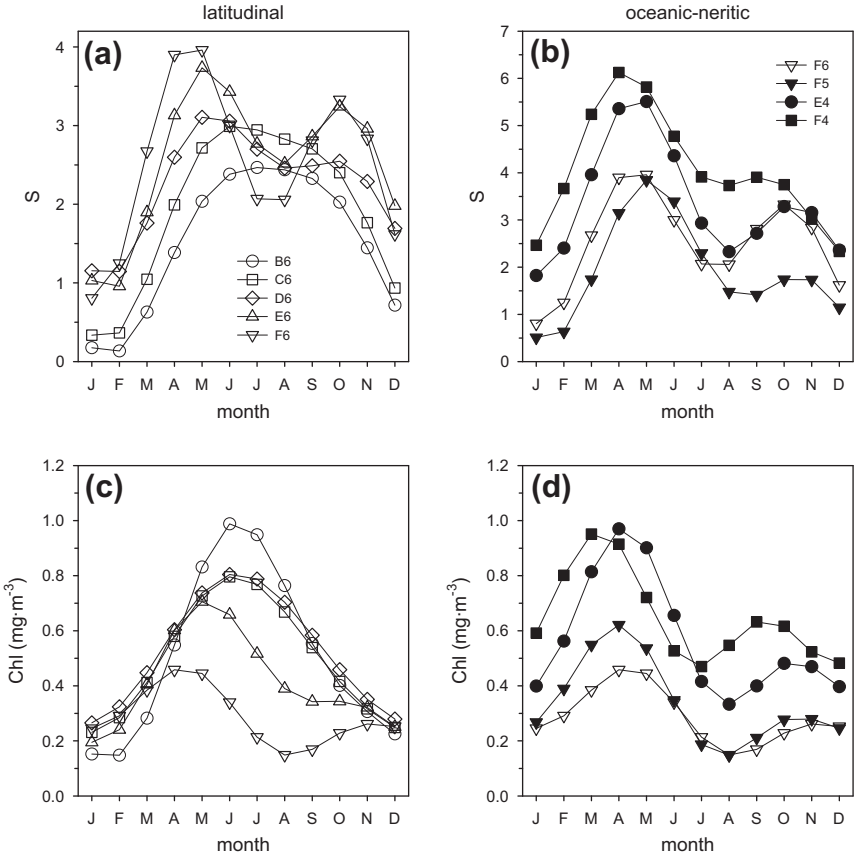

Fig. 3. Seasonal cycles (first and second harmonics of the annual period) of: (a and b) copepod species richness (S, mean number of copepod categories per CPR sample) and (c and d) surface chlorophyll from SeaWiFS (Chl, mg m^{-3}), along latitudinal (left, B6–F6) and oceanic–neritic gradients (right, F6–F4 and E4).

oceanic (F6) and neritic (F4) extremes, and the seasonal peak occurs in early February.

3.2. Species-samples curves and relationships between diversity indices (S and S_{ac})

Species-samples curves for each CPR Standard Area were obtained from the total richness per month (S_{ac}) as a function of the volume sampled by the CPR (V, m^3) that month (Fig. 4a and b). Table 3 compiles the parameter values of the fitted accumulation curves (Michaelis–Menten type: M–M). The asymptotic value of the M–M function, the maximum richness sampled by the CPR (S_{ac_max}), increased equatorward from ca. 12 to 31 taxa, but decreased from oceanic to neritic environments (23 and 20 taxa in E4 and F4 respectively). The initial slope of the fitted M–M functions (b_0 in Table 3), however, increased along both gradients, equatorward (from 0.09 to 0.24 in B6 and F6 respectively) and towards neritic environments (from 0.24 to 0.37 in F6 and F4 respectively).

In order to check to what extent S_{ac} (and S_{ac_max}) values derived from the CPR could provide an estimation of the actual (and maximum) values of species richness, we have compared the species-samples curve obtained in F4 during April with values of species richness of calanoid copepods obtained in this area and month using conventional net sampling methods (Fig. 4c). The three datasets used for comparative purposes come from two different sources: the monthly time-series monitoring programme RADIALES (http://www.seriestemporales-ieo.net) for the sections off A Coruña (43.4°N, 8.4°W; Northwest Iberian shelf; from 1994 to 2006; vertical hauls down to a maximum depth of 100 m with WP2 of 200 μm mesh size) and Santander (43.5°N, 3.8°W, Central Cantabrian shelf, from 1991 to 1996; double oblique hauls down to a maximum depth of 50 m with Juday–Bogorov net of 250 μm mesh size) (Valdés and Moral, 1998), and an extensive sampling carried out in April 2004 all along the Northwest and North Iberian shelf (similar sampling protocols that in the section off A Coruña) (Cabal et al., 2008) (details of datasets in caption of Fig. 4c). The comparison between the values of S_{ac} from the CPR and of species richness from the three independent datasets is reasonably good considering the differences between sampling methods (devices, mesh-sizes, epipelagic versus water column integrated, etc.). The relationship between the monthly cumulative richness (S_{ac}) and mean richness per sample (S) could be represented by a saturating M–M function (Fig. 4d). The fitted function accounted for 60% of the variability, and its parameters, maximum richness (S_{ac_max}) and mean richness at half S_{ac_max}, were ca. 44 and 5 copepod categories.

3.3. Relationship between mean taxonomic richness (S) and environmental variables

On the year-to-year scale (Fig. 5a–d), the correlation between the de-trended (Table 4) annual averages of S and surface chlorophyll (Chl) was significant along the latitudinal gradient ($r = -0.48$, $p < 0.01$, $n = 28$), but not along the oceanic–neritic gradient or when the data from both gradients were pooled (Fig. 5a and Table 5). S showed a positive linear relationship with the index of seasonality of phytoplankton standing stock (SPSS) along both gradients ($r = 0.40$, $p < 0.01$, $n = 46$), but not when the data for each gradient were considered separately (Fig. 5b, Table 5). The de-trended annual averages of S and sea surface temperature (SST) showed a highly significant ($p < 0.001$) positive

Table 2
As in Table 1 but for the environmental variables: chlorophyll concentration from SeaWiFS (Chl, mg·m^{-3}) for the period 1998–2008; sea surface temperature (SST, °C) (1948–2007); number of days per month with daily averaged wind speed exceeding 10 m s^{-1} (w10, days·month^{-1}) (1950–2007). For Chl, the number of samples (n) corresponds to the number of pixels (9×9 km^2) within each CPR SA multiplied by the number of available monthly data. For SST and w10, n indicates the number of time series data (monthly or daily respectively) and of grid points averaged within each CPR Area (in brackets).

Var	CPR Area	n mo	$\bar{x}$	b	EV_{LT}	T	A	F	T_m	EV_{SC}	Φ_1	EV_{AR}	EV_T
Chl	B6	6912	0.51			12	0.40	2.80	6.7	59.9	0.31	3.5	66.6
		94				6	0.09	0.11	5.9	3.3			
	C6	6912	0.50			12	0.28	2.91	6.4	47.8	0.52	14.2	62.4
		96				6	0.03	0.49	5.5	0.4			
	D6	8640	0.53			12	0.27	2.89	6.5	51.0	0.54	14.4	65.6
		111				6	0.02	0.66	5.4	0.2			
	E6	8640	0.41	−0.02	7.4	12	0.21	3.29	5.7	39.9	0.48	10.3	66.9
		121				6	0.10	1.15	4.9	9.3			
	F6	8640	0.29	−0.01	8.0	12	0.12	4.33	3.7	29.5	0.56	15.7	64.6
		122				6	0.07	1.44	4.6	11.3			
	F5	7200	0.34	−0.01	2.9	12	0.18	4.42	3.6	44.2	0.23	1.7	66.7
		122				6	0.11	1.95	4.1	17.9			
	E4	3024	0.57			12	0.24	4.15	4.1	36.3	0.47	10.6	63.6
		120				6	0.17	1.82	4.3	16.7			
	F4	2100	0.65	0.01	1.6	12	0.16	4.57	3.3	22.0	0.35	7.4	50.8
		122				6	0.15	2.79	3.3	19.8			
SST	B6	720 (×12)	9.03	0.004	0.09	12	1.97	2.02	8.1	84.0	0.79	4.1	88.2
		720				6	0.56	4.40	1.8	6.9			
						720	0.39	5.62	75.6	3.3			
	C6	720 (×12)	10.26	0.004	0.01	12	2.14	1.96	8.3	86.5	0.74	3.6	90.1
		720				6	0.49	4.31	1.9	4.5			
						720	0.39	5.80	55.5	2.9			
	D6	720 (×12)	12.07	0.003	0.08	12	2.40	1.97	8.2	86.7	0.69	3.6	90.3
		720				6	0.50	4.21	2.0	3.7			
						720	0.36	6.18	11.4	1.9			
	E6	720 (×18)	14.20			12	2.65	1.95	8.3	86.8	0.64	2.9	89.6
		720				6	0.62	4.16	2.0	4.8			
						720	0.35	0.22	694.6	1.5			
	F6	720 (×18)	17.13			12	3.39	1.90	8.4	91.4	0.61	1.3	92.7
		720				6	0.71	4.10	2.1	4.0			
						720	0.38	0.38	676.3	1.1			
	F5	720 (×15)	16.50			12	3.22	1.87	8.4	93.4	0.65	1.2	94.6
		720				6	0.53	4.02	2.1	2.6			
						720	0.36	0.44	669.6	1.1			
	E4	720 (×10)	14.24	0.003	0.36	12	3.52	1.95	8.3	93.7	0.66	1.1	95.1
		720				6	0.60	4.30	1.9	2.8			
						720	0.33	0.50	662.8	0.8			
	F4	720 (×7)	16.10			12	3.03	1.91	8.4	92.7	0.60	1.5	94.2
		720				6	0.42	4.06	2.1	1.8			
						720	0.37	0.54	658.1	1.4			
w10	B6	20 805 (×10)	12.32	0.03	0.5	12	6.77	5.82	0.9	63.5			64.0
		696				6	1.02	2.76	3.4	1.4			
	C6	20 805 (×10)	14.48	0.02	0.4	12	6.22	5.90	0.7	56.5			56.8
		696				6	0.81	2.49	3.6	1.0			
	D6	20 805 (×15)	13.83			12	6.08	5.93	0.7	54.3			54.3
		696				6	0.52	1.60	4.5	0.4			
	E6	20 805 (×15)	11.88	0.03	0.7	12	6.49	5.81	0.9	56.6			57.3
		696				6	0.43	1.14	4.9	0.3			
	F6	20 805 (×15)	8.69	0.03	0.7	12	6.47	5.70	1.1	56.3			56.9
		696				6	0.56	1.18	4.9	0.4			
	F5	20 805 (×12)	8.67	0.03	0.8	12	4.95	5.68	1.2	43.1			43.9
		696				6	0.79	1.23	4.8	1.1			
	E4	20 805 (×6)	8.12	0.02	0.5	12	5.43	5.81	0.9	51.7			52.2
		696				6	0.58	0.62	5.4	0.6			
	F4	20 805 (×2)	1.46			12	1.88	5.86	0.8	32.5			32.5
		696				6	0.53	5.64	0.6	2.6			

correlation along the latitudinal gradient ($r = 0.62$, $n = 96$) or when all the data are pooled ($r = 0.64$, $n = 180$), but not when only the data along the oceanic–neritic gradient were considered (Table 5; Fig. 5c). There was no relationship between the de-trended annual averages of S and the number of days per month with daily average wind speed exceeding 10 m s^{-1} (w10) along the latitudinal gradient, but a highly significant ($p < 0.001$) negative linear relationship along the oceanic–neritic gradient ($r = -0.38$, $p < 0.001$, $n = 95$) or when the data for both gradients were pooled ($r = -0.69$, $p < 0.001$, $n = 180$) (Fig. 5d).

At the climatological scale, the correlation between the climatological averages of S and Chl was not significant (Fig. 5e, Table 6). Significant positive correlations were found with the SPSS index ($r = 0.97$, $p < 0.001$, $n = 6$) (Fig. 5f) and to a lesser extent with SST ($r = 0.76$, $p < 0.05$, $n = 7$) (Fig. 5g), although in this last case the general relationship between S and SST was forced by the latitudinal gradient. The relationship between S and w10 was also significant but negative ($r = -0.90$, $p < 0.01$, $n = 7$) (Fig. 5h). According to these results, the best predictor of the geographic variation of the climatological average of S was the climatological average of the SPSS index. The regression line obtained (Table 6) was applied to map the expected climatological average of S as a function of the average value of SPSS in each SeaWiFS pixel (area of 9×9 km^2) of the North Atlantic (between latitudes 30° and 70°N and longitudes

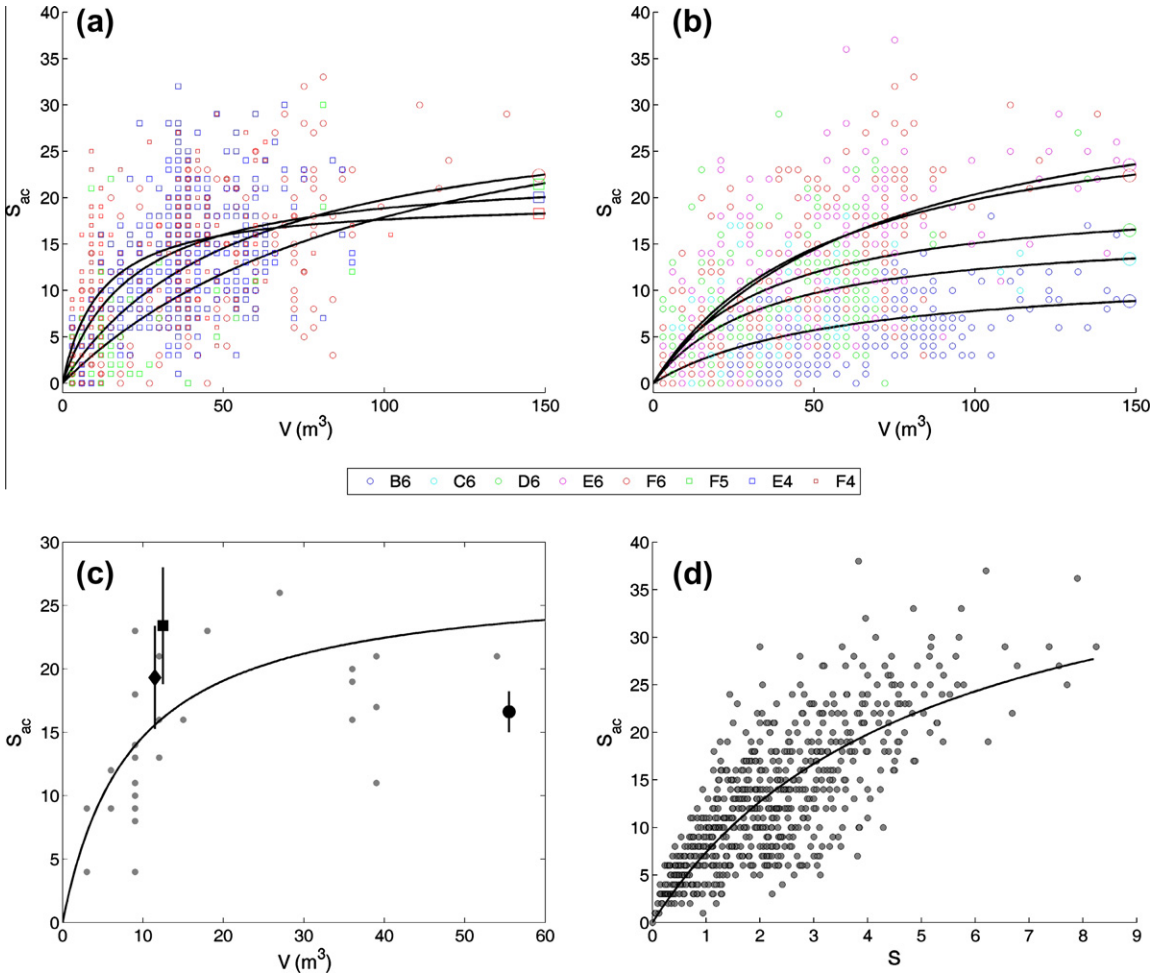

Fig. 4. Species-samples curves for each CPR Standard Area derived from the relationship between the cumulative number of copepod categories per month (S_{ac}) and the sampled volume (V, m^3; V = number of CPR samples × 3 m^3·sample^{-1}), along (a) latitudinal and (b) oceanic–neritic gradients; the assignment of each accumulation curve to its corresponding CPR Standard Area is indicated by a larger symbol at the extreme of the fitted function (Table 3). (c) Accumulation curve for April in F4 (North Iberian shelf) from CPR data (grey dots, n = 27) and for three independent data sets obtained by conventional net sampling methods in a mid-shelf oceanographic station off A Coruña (closed diamond) and Santander (closed circle) (monthly time series monitoring programme RADIALES), and a grid of stations distributed all along the Northwest and North Iberian shelf (PELACUS cruise of 2004; closed square). The statistics of copepod species richness for these independent data sets are: time series off A Coruña, n = 12 (monthly between 1994 and 2006), V = 13 m^3, mean S_{ac} = 19.3, min. S_{ac} = 15, max. S_{ac} = 29; time series off Santander, n = 5 (monthly between 1992 and 1996), V = 56 m^3, mean S_{ac} = 16.7, min. S_{ac} = 14, max. S_{ac} = 18; extensive sampling, n = 98, V = 13 m^3, mean S_{ac} = 23.4, min. S_{ac} = 14, max. S_{ac} = 33. (d) Relationship between the cumulative number of species per month (S_{ac}) and monthly mean copepod species richness per CPR sample (S); the parameters of the Michaelis–Menten relationship between S_{ac} and S are: S_{ac_max} = 44 ± 6, S_M = 5 ± 1 (n = 706, r^2 = 0.60, p < 0.001).

Table 3
Parameters of the accumulation curves (Michaelis–Menten type) fitted to the relationship between total richness per month (S_{ac}) and sampled volume (V, m^3) for the selected CPR Standard Areas (CPR Area). Abbreviations stand for: n, number of samples (months); S_{ac_max}, maximum (asymptotic) value of S_{ac}; V_M, constant of the saturating function (i.e. value of V at which S_{ac} equals ½ S_{ac_max}); r^2, coefficient of determination of the fitted function. The initial slope of the Michaelis–Menten function is also given (b_0, copepod categories·m^{-3}). All relationships are significant at p < 0.001.

CPR area	n	Michaelis–Menten function			b_0 ± SE
		S_{ac}_max ± SE	V_M ± SE	r^2	
B6	453	12 ± 3	58 ± 45	0.19	0.09 ± 0.01
C6	166	17 ± 5	36 ± 21	0.46	0.18 ± 0.02
D6	233	21 ± 5	37 ± 22	0.39	0.21 ± 0.01
E6	192	35 ± 9	71 ± 36	0.45	0.22 ± 0.02
F6	148	31 ± 11	56 ± 43	0.32	0.24 ± 0.02
F5	68	37 ± 40	105 ± 160	0.30	0.24 ± 0.04
E4	515	23 ± 4	22 ± 10	0.16	0.35 ± 0.01
F4	365	20 ± 2	12 ± 8	0.41	0.37 ± 0.02

60°W to 5°E) (Fig. 6). Within the analysed spatial domain (framed area in Fig. 6), the expected values of the climatological averages of S capture the main geographic patterns described: the increasing pattern equatorward and towards neritic environments. However, the finer spatial scale of the explanatory variable (i.e. average SPSS in each SeaWiFS pixel) impose considerable regional to mesoscale variability in the spatial distribution of S, such as the patchiness in the oceanic environment at about 40°N, the differences between the western and northern Iberian shelf, the high values associated to the oceanic margin of the French shelf and the low values in the central part of the Bay of Biscay.

3.4. Role of meteo-hydrographic variability and disturbances

The distribution of the annual residuals of S versus those of SST ($\Delta S_{j,k}$:$f(\Delta SST_{j,k})$, Eq. (6.2)) along the latitudinal gradient described a double bell-shaped pattern, with peaks of species richness at ΔSST around −0.4 and +0.5 °C and species richness values close to the climatological average of its respective CPR Standard Area ($\Delta S \sim 0$) when the annual residuals of temperature are close to zero (Fig. 7a). The distribution showed a unimodal pattern when the annual anomalies of S were related with the absolute values of the an-

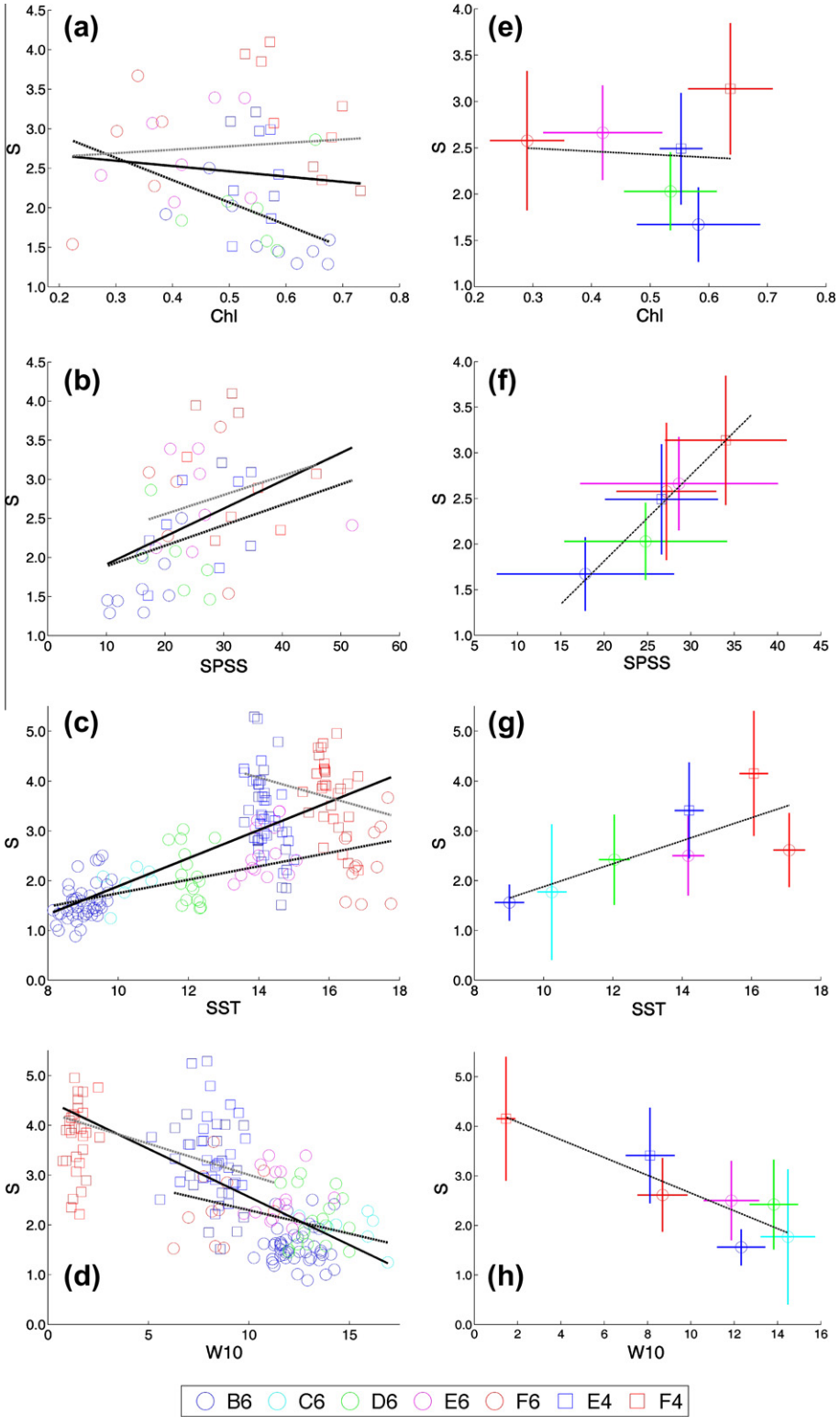

Fig. 5. Relationships between mean copepod species richness per sample (S) and environmental variables at year-to-year (left figures) and climatological (right figures) scales; (a and e) surface chlorophyll (Chl, mg m^{-3}); (b and f) index of seasonality of phytoplankton standing stock (SPSS = 100·Chl$_{min}$/Chl$_{max}$); (c and g) sea surface temperature (SST, °C); (d and h) number of days per month with daily averaged wind speed exceeding 10 m s^{-1} (w10, days month^{-1}). For the year-to-year relationships, the linear regressions along the latitudinal (dotted), oceanic–neritic (grey) and both gradients (black) are shown (Table 5). For the relationships between the climatological averages, the bars indicate the standard error of the mean and the dotted line the linear regression (Table 6).

nual anomalies of SST (peak at |ΔSST| about 0.4–0.5 °C) (Fig. 7b). The relationship between the anomalies of these variables for the CPR Standard Areas with higher neritic influence (E4 and F4, Fig. 8a and b) was similar, with peaks of ΔS at ca. −0.5 and +0.2 °C respectively. The bell-shaped pattern also held when considering the absolute values of ΔSST:ΔS peaked at |⊿SST| values about 0.2 °C (Fig. 8b).

Table 4
Slope of the linear trend of the time series of the annual averages of mean copepod species richness per sample (S) and environmental conditions (Chlorophyll, Chl, for 1998–2006 and SST and w10 for the period 1958–2006). The number of valid years (i.e. more than six sampled months per year) of S in each of the analysed CPR boxes is indicated in column n. The asterisks indicate the significance level of the trend.

CPR Area	n	S	Chl	SST	w10
B6	45	−0.001	0.003	−0.006	0.026**
C6	7	−0.007	0.005	−0.004	0.024*
D6	18	−0.005	0.000	−0.001	0.010
E6	15	0.008	−0.019**	0.001	0.028**
F6	11	0.020	−0.013**	0.001	0.024**
F5	2	–	−0.0010*	0.004	0.026**
E4	49	−0.047***	0.007	0.005	0.023**
F4	35	−0.048***	0.010*	0.002	0.007

No asterisk indicates that the trend is no significant.
* $p < 0.05$.
** $p < 0.01$.
*** $p < 0.001$.

The distribution of the annual residual of S described also a double bell-shaped pattern in relation to the annual residuals of the number of days per month with daily average wind speed exceeding 10 m s^{-1} (w10). The peaks of species richness occurred at values of Δw10 around −1 and +1 days per month, and species richness values were close to its respective climatological average for values of $\Delta w10 \sim 0$, both for data along the latitudinal gradient (Fig. 7c) and from the neritic environments (Fig. 8c). A unimodal relationship was also obtained between the annual anomalies of S and $|\Delta w10|$: the peak took place at $|\Delta w10|$ between 1 and 1.5 days per month for the data along the latitudinal gradient (Fig. 7d) and around 1 day per month for the data from the neritic environments (Fig. 8d).

4. Discussion

4.1. Time series analysis and the estimation of species richness

Two methodological considerations must be taken into account before interpreting the results presented here. First, although the application of time series analysis methods on spatial compartments have been and still are (e.g. Kirby et al., 2009) commonly applied to CPR data in order to extract the components of variability of the series (e.g. overview of statistical methods by Beaugrand et al., 2003; Beare et al., 2003) biases may arise as a result of the possible interaction between temporal components and between those and spatial processes such as spatial autocorrelation (Beaugrand and Ibañez, 2002). In a series of papers published in recent years, Beaugrand and colleagues have combined multivariate, time series and geostatistical tools to tackle satisfactorily these problems (e.g. Beaugrand et al., 2000a). The good comparability between the species richness patterns obtained by Beaugrand et al. (2002b) and those obtained by us (see below) suggests that the application of conventional time series analysis methods on spatial compartments, such as the CPR Standard Areas, renders satisfactory results in terms of description of the main temporal components and their spatial variability. Furthermore, the combination of time series analysis on spatial compartments and regression techniques is a suitable way to infer the functional relationship between variables.

Table 6
Parameters of the linear regression between the climatological averages in each CPR Standard Area of mean copepod species richness per sample (S) and environmental conditions (Chlorophyll, Chl; index of seasonality of phytoplankton standing stock, SPSS; sea surface temperature, SST; number of days per month with daily average wind speed exceeding 10 m s^{-1}, w10). n, number of CPR Standard Areas; b, slope of the linear trend; a, ordinate at origin; r, correlation coefficient; α, significance level of the fitted linear function.

Variable	n	b	a	r	α
Chl	6	−0.32 ± 5.70	2.59 ± 2.89	−0.08	0.87
SPSS	6	0.094 ± 0.031	−0.071 ± 0.841	0.97	0.001
SST	7	0.23 ± 0.22	−0.43 ± 3.06	0.76	<0.05
w10	7	−0.179 ± 0.102	4.44 ± 1.11	−0.90	<0.01

The second consideration is related with the indices of species richness used to analyse the patterns of diversity and their underlying causes. The mean taxonomic richness per CPR sample proposed by Beaugrand et al. (2000b) 'should be considered more as an index of diversity than the actual number of taxa'. According to Magurran (2004), in studies concerning the changes in species composition along environmental gradients (i.e. beta- or gamma-diversity), diversity indices that emphasise the number of taxa (species richness) are more suitable than those that weight other components of diversity such as the distribution of abundance within taxa (evenness) or the relatedness of different taxa (distinctness) (Purvis and Hector, 2000). On the other hand, the cumulative richness per month (S_{ac}) derived from CPR data provides reasonably estimations of the 'actual' number of species (copepod categories), at least comparable with those obtained by conventional net sampling methods (Fig. 4c). As expected, S_{ac} values fit a saturating function of the sampled volume (Gotelli and Colwell, 2001). It can be argue to what extent the parameters of the

Table 5
Parameters of the linear regression between the annual averages of the mean copepod species richness per sample (S) and environmental conditions (Chlorophyll, Chl; index of seasonality of phytoplankton standing stock, SPSS; sea surface temperature, SST; number of days per month with daily average wind speed exceeding 10 m s^{-1}, w10). The linear functions were fitted to data along the latitudinal and oceanic–neritic gradients separately and to all the data pooled (both). Only those years with more than six sampled months were used to estimate the annual averages of S. The annual time series were de-trended if necessary prior to the estimation of the linear regression (Table 4). n, number of years; b, slope of the linear trend; a, ordinate at origin; r, correlation coefficient; α, significance level of the fitted linear function.

Variable	Gradient	n	b	a	r	α
Chl	Latitudinal	28	−2.52 ± 2.00	3.40 ± 1.05	−0.48	0.01
	Oceanic–neritic	23	0.43 ± 2.42	2.56 ± 1.37	0.17	0.41
	Both	46	−0.64 ± 1.96	2.67 ± 1.05	−0.05	0.73
SPSS	Latitudinal	28	0.026 ± 0.034	1.62 ± 0.80	0.29	0.12
	Oceanic–neritic	23	0.017 ± 0.043	2.31 ± 1.16	0.17	0.42
	Both	46	0.036 ± 0.025	1.55 ± 0.16	0.40	<0.01
SST	Latitudinal	96	0.13 ± 0.35	0.39 ± 0.40	0.62	<0.001
	Oceanic–neritic	95	−0.08 ± 0.20	4.8 ± 3.05	−0.09	0.39
	Both	180	0.28 ± 0.05	−0.93 ± 0.65	0.64	<0.001
w10	Latitudinal	96	−0.06 ± 0.06	2.69 ± 0.78	−0.19	0.06
	Oceanic–neritic	95	−0.13 ± 0.06	4.26 ± 0.41	−0.38	<0.001
	Both	180	−0.19 ± 0.03	4.49 ± 0.30	−0.69	<0.001

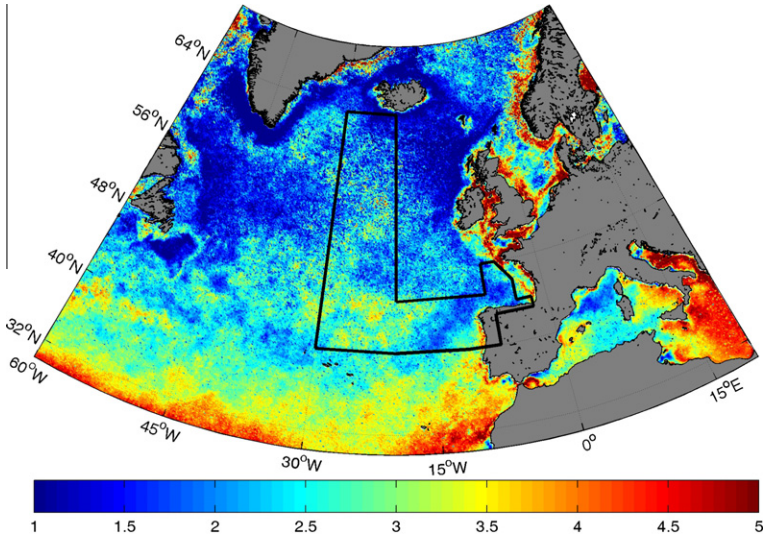

Fig. 6. Geographic variation of the climatological average of S derived from the application of the linear regression fitted to the relationship between the climatological averages of S and the index of seasonality of phytoplankton standing stock (SPSS) (Fig. 5f, Table 6). The values of the average SPSS index were calculated for each SeaWiFS pixel (are of 9×9 km^2). The frame indicates the spatial domain analysed.

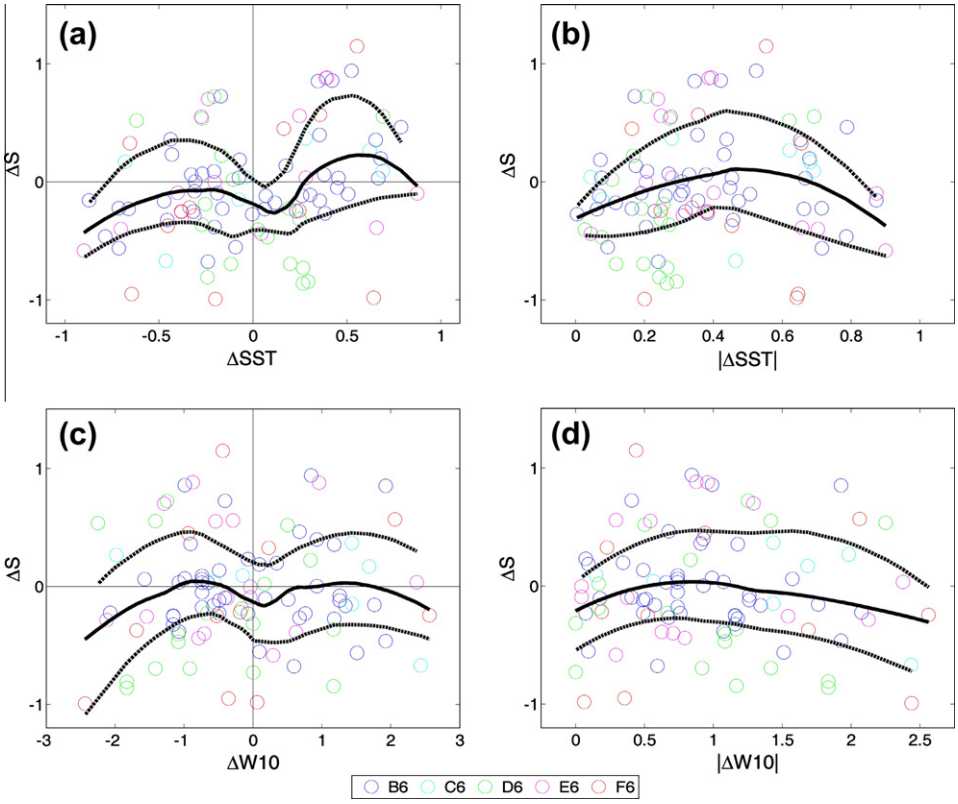

Fig. 7. Relationship between the annual anomalies of mean copepod species richness per CPR sample (S) and annual anomalies of the meteo-hydrographic environment for the CPR Standard Areas along the oceanic latitudinal gradient (B6–F6): (a) sea surface temperature (ΔSST, °C); (b) absolute values of the anomalies of SST; (c) number of days per month with wind speed exceeding 10 m s^{-1} (Δw10, days month^{-1}); (d) absolute values of w10. The lines depict the loess function fitted to the average and to the 1st and 2nd quartiles of the distribution.

saturating function fitted to the species-samples curves, here a Michaelis–Menten type, provide meaningful information. We have shown that both the maximum richness (S_{ac_max}) and the initial slope (b_0) increased equatorward along the latitudinal gradient (Fig. 4a). However, along the oceanic–neritic gradient b_0 displayed the expected pattern (steeper slope as one moves toward neritic environments) while S_{ac_max} did not (Fig. 4b). A close inspection of the relationship between S_{ac} and sampled volume along this gradient shows that this contradictory result could arise from a poor definition of the accumulation curves, and hence a misfit of the M–M function, due to the scarcity of samples (as it is the case for F5), the relatively narrow range of sample volumes (E4 and F4), or the distribution of samples around two separate centroids (F4, S_{ac} values around 10 and 40 m^3 of sample volume probably owing

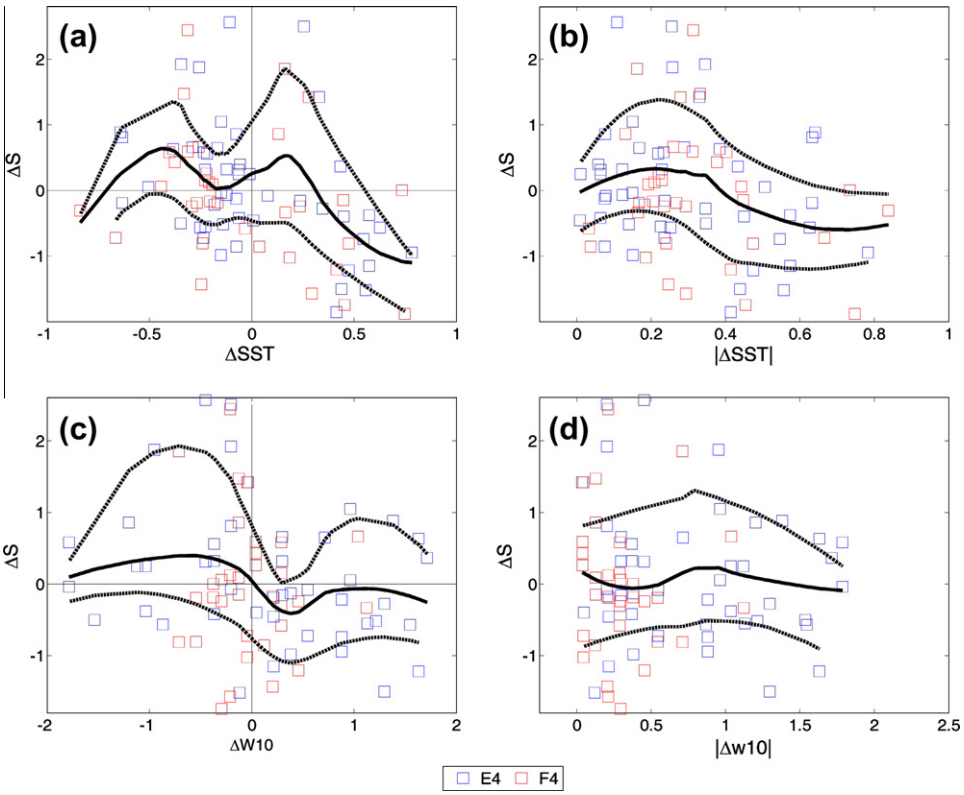

Fig. 8. As in Fig. 7 but for the CPR Standard Areas with more neritic features (E4 and F4).

to the routes taken by the 'ships of opportunity' within this CPR Standard Area) (Richardson et al., 2006). Thus, accumulation curves could supply valuable information provided that the number and distribution of species-samples data is appropriate, which applied to CPR data imply a sufficient number of data and a relatively wide range of sample volumes. The relationship between S_{ac} and S allow us to infer the 'actual' richness from the mean taxonomic richness per sample. This relationship could be useful for comparative purposes. For instance, using the relationship between S_{ac} and S we obtain values of S_{ac} from ca. 10 to 15 along the oceanic latitudinal gradient. Wood-Walker et al. (2002), using data from the Atlantic Meridional Transects (AMT), reported for the Atlantic Ocean an equatorward increment of taxonomic richness of epipelagic (0–200 m) copepod genera sampled with WP2 of 200 μm mesh-size from ca. 7 to 18 between latitudes 60° and 30° N, which compares reasonably well with the (cumulative) number of copepod categories sampled by the CPR (S_{ac}).

4.2. Patterns of species richness along latitudinal and oceanic–neritic gradients

The climatological average of mean taxonomic richness per CPR sample (S) increases equatorward along the latitudinal gradient and towards neritic environments along the oceanic–neritic gradient. Both the slope of the increment along these gradients and the climatological averages in each of the CPR Standard Areas were similar to those reported by Beaugrand et al. (2000b) using the same data source but a different numerical analysis approach. Equatorward increments in copepod diversity have been also reported by Wood-Walker et al. (2002) and Rombouts et al. (2009). The latter also analysed the longitudinal variation of diversity but did not find significant patterns.

Seasonality is a prominent mode of variation in the study region and has been the focus of numerous investigations in relation to zooplankton abundance (e.g. Colebrook and Robinson, 1965; Colebrook, 1979), autecology (e.g. Hays et al., 1995; Planque and Batten, 2000), community assemblages (e.g. Colebrook et al., 1961; Beaugrand et al., 2000a) and diversity (Beaugrand et al., 2001). The geographic pattern of variation of the seasonality of S is similar to that inferred by Beaugrand et al. (2000a, 2001). The seasonality of species richness increases its bi-modal character equatorward, shaping a single summer peak in boreal latitudes and a main spring and a secondary autumn peak, with a relative decrease in summer, in temperate latitudes. The differences between these two seasonal modes occur between 50° and 55°N (CPR Standard Area D6), which is in agreement with the transition between the Southeast and Northern North Atlantic Drift Provinces at 53°N (Beaugrand et al., 2001). The first peak of diversity takes place progressively earlier equatorward: between April–May in oceanic temperate latitudes (F6–E6–D6) and two months later (June–July) in boreal latitudes (C6–D6). The peak of S is almost coincidental with the spring bloom of phytoplankton at temperate locations but it is about 1–2 months lagged in boreal latitudes (Fig. 5). Possible explanations for the uncoupling between copepod diversity and phytoplankton outburst at boreal latitudes include the effect of temperature on the growth of copepods (Carlotti et al., 1993), physical processes (advection and mixed layer depth dynamics) (Planque et al., 1997) and food availability (Richardson and Verheye, 1999; Beaugrand et al., 2001).

At temperate latitudes, in both oceanic and neritic environments, the secondary autumn peak in diversity that occurs around October is also coupled with the autumn phytoplankton bloom. This bloom is the result of de-stratification of the water column and the resulting injection of nutrients into surface waters, thus relaxing the oligotrophic conditions that prevail during summer (Nogueira et al., 2006). Along the oceanic–neritic gradient, the variance explained by the seasonal cycle is lower and the timing of diversity occurs earlier in neritic than in oceanic environments.

Angel (1997) suggested that in neritic environments, the interaction between the morphology of oceans margins and the variety of physical processes occurring at the mesoscale leads to a finer-scaled structuring of the environment that may promote higher diversity. Mesoscale processes, such as coastal upwelling and associated filaments, continental runoff and river plumes, eddies, and tidal, buoyancy and slope currents, are recurrent features in the North Iberian shelf and Bay of Biscay areas (F4 and E4) (Koutsikopoulus and Le Cann, 1995).

Beaugrand et al. (2002b) pointed out a poleward expansion of warm-water assemblages (southern shelf edge and pseudo-oceanic temperate species) and a retreat of cold-water assemblages (cold-temperate and subarctic species) in the North Atlantic, particularly noticeable in the British Isles and North Sea. Our analysis revealed significant long-term trends of copepod diversity, increasing in the northernmost area (B6) between 1991 and 2006 and decreasing in the Bay of Biscay and North Iberian shelf (E4 and F4) during the period 1958–2006. Close inspection of the time series of individual taxa for these south-eastern areas presents some interesting features. The occurrence of several taxa showed an apparent decreasing tendency, evaluated as the ratio between the percentages of presence in the first and second halves of the series (1958–1980 versus 1981–2006). Most of them belong to warm-temperate (*sensu* Beaugrand et al., 2002a,b) (*Calocalanus* spp., *Nannocalanus minor*, *Pleuromamma abdominalis* and *Pleuromamma borealis* decreased in both areas) or subtropical (*Lucicutia* spp., *Eucalanus elongatus* and *Centropages violaceus* decreased in E4) oceanic species associations. There are also several species that showed and increasing tendency in both areas (*Calanus finmarchicus*, *Ctenocalanus vanus* and *Anomalocera patersoni*, representatives of subarctic, southern shelf edge and coastal associations respectively) or only in E4 (*Temora stylifera* and *Euchaeta gracilis*, representatives of subtropical and southern shelf edge associations respectively). The fact that the majority of the taxa involved in the decrease of mean taxonomic richness belong to warm-temperate and subtropical associations, despite the warming trend observed in the Bay of Biscay and North Iberian shelf in the last decades (between 1958 and 2007) (deCastro et al., 2009), suggest that other factors rather than the direct effect of temperature need to be considered to explain the observed trends in species richness. Changes in the strength of physical processes, such the intensification of the slope current (Iberian Poleward Current) in the last two decades (1986–2007) (González-Nuevo and Nogueira, 2005) or the weakening of the intensity of coastal upwelling in the last four (1965–2006) (Pérez et al., 2010), have been observed in the Iberian shelf. The observed trends in the intensity of these physical processes could affect copepod diversity by promoting a decrease of productivity and a shift in the phytoplankton community involving a relative reduction of diatoms and an increase of dinoflagellates (Álvarez-Salgado et al., 2003; Pérez et al., 2010).

4.3. Underlying factors

The positive latitudinal relationship between temperature and species richness for an ample number of taxa, both for marine and terrestrial organisms (e.g. Rohde, 1992; Roy et al., 1998; Rutherford et al., 1999; Macpherson, 2002; Hillebrand, 2004; Rombouts et al., 2009), gives support to the species richness–energy hypothesis (Wright, 1983). According to this hypothesis, available energy, or one of the multiple surrogate parameters used for energy, affects richness through the physiological response to temperature (Willing et al., 2003). Besides the direct effect of temperature on individual metabolic rates and generation times, temperature in the pelagic environment is an indicator of physical processes that may affect diversity. For instance, the variability of temperature associated to the dynamics of the thermocline, which exerts a major role on phytoplankton production (Sverdrup, 1953), could be a proxy for the chemical energy available to fuel secondary production (Rombouts et al., 2009). Several authors have found a negative relationship between stratification and zooplankton biomass (Roemmich and McGowan, 1995) and diversity (Valdés and Moral, 1998). The rationale for this negative relationship is that stratification hampers the surface enrichment of nutrients from deeper layers, limiting phytoplankton growth and thus the availability of food for zooplankton. The magnitude and sign of these relationships, however, may be different depending on the turbulence-nutrient regime of the region of interest. For instance, the increase of sea surface temperature (SST) in boreal, turbulent–nutrient-rich cool waters, may promote an increment of phytoplankton and zooplankton biomass through the direct effect of temperature on metabolic rates (Richardson and Schoeman, 2004). In our study, sea surface temperature (SST) and copepod species richness (S) co-varied along the latitudinal gradient, and SST is indeed a good predictor of S along this gradient, but not along the oceanic–neritic gradient (Fig. 5c and g), suggesting that other factors must be taken into consideration in this case.

The values of S were related at climatological and year-to-year scales with the index of seasonality of phytoplankton standing stocks (SPSS index, defined as the ratio between the monthly minimum and maximum surface chlorophyll) (Fig. 5b and f). The positive linear relationship between S and the SPSS index predicts that 'species richness decreases (and dominance increases) as organic inputs become more seasonally pulsed' (Angel, 1997). The amplitude of production cycles decreases equatorward (Longhurst, 1998) (i.e. higher values of the SPSS index); production is almost continue through the year and primary and secondary production are closely coupled. This produces a retentive system (i.e. closed biogeochemical cycles through tight coupling between ecosystem components) which promotes high diversity (Longhurst and Pauly, 1987). In contrast, production and consumption become increasingly uncoupled poleward promoting lower diversity (Wood-Walker et al., 2002). The near match between seasonality of S and Chl at temperate latitudes in contrast with the mismatch at boreal latitudes (Fig. 5) supports this reasoning and the relevance of the species richness–productivity hypothesis on the control of copepod diversity. From the relationship between the climatological averages of S and SPSS (Fig. 5f, Table 6) we mapped the distribution of copepod species richness in the North Atlantic (Fig. 6). Our results show striking similarities with those obtained by Beaugrand et al. (2000b) taking into account that we have estimated S from the values of SPSS derived for each SeaWiFS pixel (area of $9 \times 9\ km^2$) while those authors estimated the distribution of S from CPR data on a coarser scale (ca. pixels of $92.6 \times 92.6\ km^2$ and a search radius of 463 km). Apart from the main geographic patterns of S (increment equatorward and towards neritic environments), Fig. 6 reflects the patchy distribution of diversity in the inter-gyre zone that separates the subpolar and subtropical gyres of the North Atlantic (oceanic realm between 40 and 45°N) (Pollard et al., 1996), presumably associated to the high mesoscale activity in this region. It also highlights hotspots of diversity in the NW Iberian shelf and in the French shelf and slope, probably linked to continental runoff and slope fronts (Lazure and Jegou, 1998), and low diversity in the central part of the Bay of Biscay and mid-shelf of the French coast, where deep mixed layers and consequently relatively low productivity takes place (Planque et al., 2006). This distribution of diversity contrasts to the high values reported by Beaugrand et al., 2000a for the whole Bay of Biscay.

We have obtained unimodal relationships between the annual residuals (i.e. factoring out the geographic pattern) of S and those of SST and the number of days per month with daily averaged wind speed exceeding $10\ m\ s^{-1}$ (Figs. 7 and 8). These unimodal relationships point out the role of intermediate disturbances on the control

of copepod species richness. According to the intermediate disturbance hypothesis, diversity increase when disturbances occur at intermediate frequencies (e.g. Nogueira et al., 2000) or intensity (Connell, 1978). Richness is maximised at intermediate frequencies and/or intensity of disturbances because successful competitors and competitively inferior pioneer species can co-exist; the former are not competitively excluded by the disturbances and the latter find opportunities to recover after disturbances. The relationship between the annual anomalies of *S* and SST may reflect direct effects of temperature, favouring those species which are physiologically better adapted to lower or higher values of SST than the average for a given location, or indirect through seasonal changes in the dynamics of the mixed layer or advection. In the case of w10, the effect of wind is also related with productivity through its direct role on water column turbulence, and hence productivity (Huisman et al., 1999).

In conclusion, our results suggest that the environmental factors interact at different temporal scales to cause the geographic variation of copepod species richness. Seasonal variation of productivity co-varied with copepod diversity at climatological, seasonal (at least for temperate latitudes) and year-to-year time scales both along the oceanic, latitudinal and the temperate, oceanic–neritic gradients, giving support to the species richness–productivity hypothesis. Sea surface temperature co-varied with diversity at the climatological and year-to-year scales along the latitudinal gradient but not along the oceanic–neritic gradient. These results are not enough to falsify the applicability of the species richness–energy hypothesis in the case of copepod diversity, but reduce to some extent its generality. Finally, copepod diversity is maximised at intermediate frequency and/or intensity of meteo-hydrographic disturbances, which presumably affect productivity through its role on mixed layer depth (stratification-mixing and turbulence) and mesoscale dynamics.

Acknowledgements

We gratefully thank the Sir Alister Hardy Foundation for Ocean Sciences responsible of the maintenance of the Continuous Plankton Recorder Survey. Special thanks to David Johns for kindly providing the CPR data requested. G.G.-N. acknowledges the 'Consejería de Educación y Cultura del Principado de Asturias' for the pre-doctoral fellowship. Thanks are also given to two anonymous referees who improved the final version of the manuscript. The authors dedicate this paper to the memory of our colleague and friend Jesús Cabal, deceased in June 2008.

Appendix A. Supplementary material

Supplementary data associated with this article can be found, in the online version, at doi:10.1016/j.pocean.2011.11.009.

References

Álvarez-Salgado, X.A., Figueiras, F.G., Pérez, F.F., Groom, S., Nogueira, E., Borges, A.V., Chou, L., Castro, C.G., Moncoiffé, G., Ríos, A.F., Miller, A.E.J., Frankignoulle, M., Savidge, G., Wollast, R., 2003. The Portugal coastal counter current off NW Spain: new insights on its biogeochemical variability. Progress in Oceanography 56, 281–321.

Angel, M.V., 1997. Pelagic biodiversity. In: Ormond, R.F.G., Gage, J.D., Angel, M.V. (Eds.), Marine Biodiversity: Patterns and Processes. Cambridge University Press, Cambridge, pp. 35–68.

Batten, S.D., Clark, R., Flinkman, J., Hays, G., John, E., Jonas, T., Lindley, J.A., Stevens, D.P., Walne, A., 2003. CPR sampling: the technical background, materials and methods, consistency and comparability. Progress in Oceanography 58, 193–215.

Beare, D.J., McKenzie, E., 1999. Connecting ecological and physical time series: the potential role of changing seasonality. Marine Ecology progress Series 178, 307–309.

Beare, D.J., Batten, S.D., Edwards, M., McKenzie, E., Reid, P.C., Reid, D.G., 2003. Summarising spatial and temporal information in CPR data. Progress in Oceanography 58, 217–223.

Beaugrand, G., 2004a. Monitoring marine plankton ecosystems. I: Description of an ecosystem approach based on plankton indicators. Marine Ecology Progress Series 269, 69–81.

Beaugrand, G., 2004b. The North Sea regime shift: evidence, causes, mechanisms and consequences. Progress in Oceanography 60, 245–262.

Beaugrand, G., Ibañez, F., 2002. Spatial dependence of calanoid copepod diversity in the North Atlantic Ocean. Marine Ecology Progress Series 232, 197–211.

Beaugrand, G., Ibanez, F., 2004. Monitoring marine plankton ecosystems. II: Long-term changes in the North Sea calanoid copepods in relation to hydro-climatic variability. Marine Ecology Progress Series 284, 35–47.

Beaugrand, G., Ibañez, F., Reid, P.C., 2000a. Spatial, seasonal and long-term fluctuations of plankton in relation to hydroclimatic features in the English Channel, Celtic Sea and Bay of Biscay. Marine Ecology Progress Series 200, 93–102.

Beaugrand, G., Reid, P.C., Ibañez, F., Planque, B., 2000b. Biodiversity of North Atlantic and North Sea calanoid copepods. Marine Ecology Progress Series 204, 299–303.

Beaugrand, G., Ibañez, F., Lindley, J.A., 2001. Geographical distribution and seasonal and diel changes in the diversity of calanoid copepods in the North Atlantic North Sea. Marine Ecology Progress Series 219, 189–203.

Beaugrand, G., Ibañez, F., Lindley, J.A., Reid, P.C., 2002a. Diversity of calanoid copepods in the North Atlantic and adjacent seas: species associations and biogeography. Marine Ecology Progress Series 232, 179–195.

Beaugrand, G., Reid, P.C., Ibañez, F., Lindley, J.A., Edwards, M., 2002b. Reorganization of North Atlantic marine copepod biodiversity and climate. Science 296, 1692–1694.

Beaugrand, G., Ibañez, F., Lindley, J.A., 2003. An overview of statistical methods applied to CPR data. Progress in Oceanography 58, 235–262.

Broekhuizen, N., McKenzie, E., 1995. Patterns of abundance for Calanus and smaller copepods in the North Sea: time-series decomposition of two CPR data sets. Marine Ecology Progress Series 118, 103–120.

Cabal, J., González-Nuevo, G., Nogueira, E., 2008. Mesozooplankton species distribution in the NW and N Iberian shelf during spring 2004: relationship with frontal structures. Journal of Marine Systems 72, 282–297.

Carlotti, F., Krause, M., Radach, G., 1993. Growth and development of *Calanus finmarchicus* related to the influence of temperature: experimental results and conceptual model. Limnology and Oceanography 38, 1125–1134.

Chatfield, C., 1992. The Analysis of Time Series, An Introduction, fourth ed. Chapman and Hall, New York, 131 pp.

Chown, S.L., Gaston, K.J., 2000. Areas, cradles and museums: the latitudinal gradient in species richness. Trends in Ecology and Evolution 15, 311–315.

Cleveland, W.S., Devlin, S.J., 1988. Locally-weighted regression: an approach to regression analysis by local fitting. Journal of the American Statistical Association 83, 596–610.

Colebrook, J.M., 1979. Continuous Plankton Records: seasonal cycles of phytoplankton and copepods in the North Atlantic Ocean and the North Sea. Marine Biology 51, 23–32.

Colebrook, J.M., Robinson, G.A., 1965. Continuous Plankton Records: seasonal cycles of phytoplankton and copepods in the North-east Atlantic and the North Sea. Bulletins of Marine Ecology 6, 123–139.

Colebrook, J.M., Glover, R.S., Robinson, G.A., 1961. Continuous Plankton Records: contribution towards a plankton atlas of the North-east Atlantic and the North Sea: General introduction. Bulletins of Marine Ecology 5, 67–80.

Colwell, R.K., Lees, D.C., 2000. The mid-domain effect: geometric constrains on the geography of species richness. Trends in Ecology and Evolution 15, 70–76.

Connell, J.H., 1978. Diversity of tropical rainforest and coral reefs. Science 199, 1304–1310.

Currie, D.J., 1991. Energy and large-scale patterns of animal and plant species richness. American Naturalist 137, 27–49.

Cury, P.M., Shyn, Y.-J., Planque, B., Durant, J.M., Fromentin, J.-M., Kramer-Schadt, S., Stenseth, N.C., Travers, M., Grimm, V., 2008. Ecosystem oceanography for global change in fisheries. Trends in Ecology and Evolution 23, 338–346.

Darwin, C.R., 1839. The Zoology of the Voyage of H.M. Ship Beagle, under the Command of Captain Fitzroy, R.N., during the years 1832 to 1836. Smith, Elder and Co., London, UK.

deCastro, M., Gómez-Gesteira, M., Álvarez, I., Gesteira, J.L.G., 2009. Present warming within the context of cooling-warming cycles observed since 1854 in the Bay of Biscay. Continental Shelf Research 29, 1053–1059.

deYoung, B., Barange, M., Beaugrand, G., Harris, R., Perry, R.I., Scheffer, M., Werner, F., 2008. Regime shifts in marine ecosystems: detection, prediction and management. Trends in Ecology and Evolution 23 (7), 402–409.

Gillooly, J.F., Allen, A.P., 2007. Linking global patterns in biodiversity to evolutionary dynamics using metabolic theory. Ecology 88, 1890–1894.

González-Nuevo, G., Nogueira, E., 2005. Intrusions of warm and salty waters onto the NW and N Iberian shelf in early spring and its relation to climate variability. Journal of Atmospheric and Ocean Science 10 (4), 361–375.

Gotelli, N.J., Colwell, R.K., 2001. Quantifying biodiversity: procedures and pitfalls in the measurement and comparison of species richness. Ecology Letters 4, 379–391.

Hardy, A.C., 1939. Ecological investigations with the continuous plankton recorder: object, plan and methods. Hull Bulletins of Marine Ecology 1, 1–57.

Hays, G.C., 1994. Mesh selection and filtration efficiency of the continuous plankton recorder. Journal of Plankton Research 16, 403–412.

Hays, G.C., Warner, A.J., Proctor, C.A., 1995. Spatio temporal patterns in the diel vertical migration of the copepod *Metridia lucens* in the Northeast Atlantic derived from the Continuous Plankton Recorder Survey. Limnology and Oceanography 40, 469–475.

Hillebrand, H., 2004. Strength, slope and variability of marine latitudinal gradients. Marine Ecology Progress Series 273, 251–267.

Huisman, J., Oostveen, P.-V., Weissing, F.J., 1999. Critical depth and critical turbulence. Two different mechanisms for the development of phytoplankton blooms. Limnology and Oceanography 44, 1781–1787.

Kirby, R.R., Beaugrand, G., Lindley, J.A., 2009. Synergistic effects of climate and fishing in a marine ecosystem. Ecosystems 12, 548–561.

Koutsikopoulus, C., Le Cann, B., 1995. Physical processes and hydrological structures related to the Bay of Biscay anchovy. Scientia Marina 60, 9–19.

Lazure, P., Jegou, A.M., 1998. 3D modelling of mesoscale evolution of Loire and Gironde plumes on Bay of Biscay continental shelf. Oceanologica Acta 21, 165–177.

Legendre, P., Legendre, L., 1998. Numerical Ecology, second ed. Elsevier Science, BV, xv + 853 pp.

Longhurst, A., 1998. Ecological Geography of the Sea. Academic Press, London.

Longhurst, A., Harrison, W., 1989. The biological pump: profiles of plankton production and consumption in the upper ocean. Progress in Oceanography 22, 47–123.

Longhurst, A.R., Pauly, D., 1987. The Ecology of the Tropical Oceans. Academic Press, Orlando, FL.

Macpherson, E., 2002. Large-scale species-richness gradients in the Atlantic ocean. Proceedings of the Royal Society B 269, 1715–1720.

Magurran, A.E., 2004. Measuring Biological Diversity. Blackwell Science Ltd., Oxford, UK.

Mauchline, J., 1998. The biology of calanoid copepods. In: Blaxter, J.H.S., Southward, A.J., Tyler, P.A. (Eds.), Advances in Marine Biology, vol. 33. Academic Press, 710 pp.

Mora, C., Robertson, D.R., 2005. Causes of latitudinal gradients in species richness: a test with fishes of the Tropical Eastern Pacific. Ecology 86, 1771–1782.

Nogueira, E., Ibañez, F., Figueiras, F.G., 2000. Effect of meteorological and hydrographic disturbances on the microplankton community structure in the Ría de Vigo (NW Spain). Marine Ecology Progress Series 203, 23–45.

Nogueira, E., Woods, J.D., Harris, C., Field, A.J., Talbot, S., 2006. Phytoplankton co-existence: results from an individual-based simulation model. Ecological Modelling 198, 1–22.

Pérez, F.F., Padín, X.A., Pazos, Y., Gilcoto, M., Cabanas, M., Pardo, P.C., Doval, M.A., Farina-Bustos, L., 2010. Plankton response to weakening of the Iberian coastal upwelling. Global Change Biology.

Piontkovski, S.A., O'Brien, T.D., Umani, S.F., Krupa, E.G., Stuge, T.S., Balymbetov, K.S., Grishaeva, O.V., Kasymov, A.G., 2006. Zooplankton and the North Atlantic Oscillation: a basin-scale analysis. Journal of Plankton Research 28, 1039–1046.

Planque, B., Batten, S.D., 2000. *Calanus finmarchicus* in the North Atlantic – the year of *Calanus* in the context of inter-decadal changes. ICES Journal of Marine Science 57, 1528–1535.

Planque, B., Hays, G.C., Ibañez, F., Gamble, J.C., 1997. Large scale spatial variations in the seasonal abundance of *Calanus finmarchicus*. Deep-Sea Research Part I 44, 315–326.

Planque, B., Lazure, P., Jegou, A.M., 2006. Typology of hydrological structures modelled and observed over the Bay of Biscay shelf. Scientia Marina 70S1, 43–50.

Pollard, R.D., Griffiths, M.J., Cunningham, S.A., Read, J.F., Pérez, F.F., Ríos, A.F., 1996. Vivaldi 1991 – a study of the formation, circulation and ventilation of Eastern North Atlantic Central Water. Progress in Oceanography 37, 167–192.

Poularikas, A.D., Seely, S., 1991. Signals and Systems, second ed. Boston PWS-KENT Publishing Company, Boston, 1015 pp.

Purvis, A., Hector, A., 2000. Getting the measure of biodiversity. Nature 405, 212–218.

Reid, P.C., Colebrook, J.M., Matthews, J.B.L., Aiken, J., Continuous Plankton Recorder Team, 2003. The Continuous Plankton Recorder: concepts and history, from Plankton Indicator to undulating recorder. Progress in Oceanography 58, 117–173.

Richardson, A.J., 2008. In hot water: zooplankton and climate change. ICES Journal of Marine Science 65, 279–295.

Richardson, A.J., Schoeman, D.S., 2004. Climate impact on plankton ecosystems in the Northeast Atlantic. Science 305, 1609–1612.

Richardson, A.J., Verheye, H.M., 1999. Growth rates of copepods in the southern Benguela upwelling system: the interplay between body size and food. Limnology and Oceanography 44, 382–392.

Richardson, A.J., Walne, A.W., John, A.W.G., Jonas, T.D., Lindley, J.A., Sims, D.W., Stevens, D., Witt, M., 2006. Using continuous plankton recorder data. Progress in Oceanography 68, 27–74.

Roemmich, D., McGowan, J., 1995. Climatic warming and the decline of zooplankton in the California current. Science 267, 1324–1326.

Rohde, K., 1992. Latitudinal gradients in species diversity: the search for the primary causes. Oikos 65, 514–527.

Rombouts, I., Beaugrand, G., Ibañez, F., Gasparini, S., Chiba, S., Legendre, L., 2009. Global latitudinal variations in marine copepod diversity and environmental factors. Proceedings of the Royal Society B 276, 3053–3062.

Rothschild, B.J., 1998. Year class strengths of zooplankton in the North Sea and their relation to cod and herring abundance. Journal of Plankton Research 20, 1721–1741.

Roy, K., Jablonski, D., Valentine, J.W., Rosenberg, G., 1998. Marine latitudinal diversity gradients: test of causal hypothesis. Proceedings of the Natural Academy of Sciences USA 95, 3699–3702.

Rutherford, S., D'Hont, S., Prell, W., 1999. Environmental controls on the geographic distribution of zooplankton diversity. Nature 400, 749–753.

Sverdrup, H.U., 1953. On conditions for the vernal blooming of phytoplankton. Journal du Conseill pour l'Exploration de la Mer 18, 287–295.

Valdés, L., Moral, M., 1998. Time-series analysis of copepod diversity and species richness in the southern Bay of Biscay off Santander, Spain, in relation to environmental conditions. ICES Journal of Marine Science 55, 783–792.

Warner, A.J., Hays, G.C., 1994. Sampling by the Continuous Plankton Recorder Survey. Progress in Oceanography 34, 237–256.

Webb, T.J., 2009. Biodiversity research sets sail: showcasing the diversity of marine life. Biology Letters 5, 145–147.

Wei, W.S.W., 1990. Time Series Analysis. Univariate and Multivariate Methods. Addison Wesley Publishing Company, Inc., Redwood City, California, 478 pp.

Willing, M.R., Kaufman, D.M., Stevens, R.D., 2003. Latitudinal gradients of biodiversity: pattern, processes, scale and synthesis. Annual Review of Ecology, Evolution and Systematics 34, 273–309.

Wood-Walker, R.S., 2001. Spatial distribution of copepod genera along the Atlantic Meridional transect. Hydrobiologia 453 (454), 161–170.

Wood-Walker, R.S., Ward, P., Clarke, A., 2002. Large-scale patterns in diversity and community structure of surface water copepods from the Atlantic Ocean. Marine Ecology Progress Series 236, 189–203.

Worm, B., Barbier, E.B., Beaumont, N., Duffy, J.E., Folke, C., Halpern, B.S., Jackson, J.B.C., Lotze, H.K., Micheli, F., Palumbi, S.R., Sala, E., Selkoe, K.A., Stachowicz, J.J., Watson, R., 2006. Impacts of biodiversity loss on ocean ecosystem services. Science 314, 787–790.

Wright, D.H., 1983. Species–energy theory: an extension of the species–area theory. Oikos 41, 496–506.